

## **General Disclaimer**

### **One or more of the Following Statements may affect this Document**

- This document has been reproduced from the best copy furnished by the organizational source. It is being released in the interest of making available as much information as possible.
- This document may contain data, which exceeds the sheet parameters. It was furnished in this condition by the organizational source and is the best copy available.
- This document may contain tone-on-tone or color graphs, charts and/or pictures, which have been reproduced in black and white.
- This document is paginated as submitted by the original source.
- Portions of this document are not fully legible due to the historical nature of some of the material. However, it is the best reproduction available from the original submission.

STAR  
143



A NOVEL ALGORITHM FOR  
SEA SURFACE HEIGHT ESTIMATION  
USING COMPLEX SAR DATA

FINAL REPORT

Period: July 1, 1982 to December 31, 1983

NASA GRANT NAGW-387

(NASA-CR-173199) [SEA HEIGHT INFORMATION  
FROM COMPLEX SAR DATA] Final Report, 1 Jul.  
1982 - 31 Dec. 1983 (Maryland Univ.) 15 p  
HC A02/MF A01 CACL 12A

N84-16872  
THRU  
N84-16875  
Unclas  
18234  
G3/64

Dr. Robert O. Harger  
Electrical Engineering Department  
University of Maryland  
College Park, Maryland 20742

D<sub>1</sub>  
N84 16873

A NOVEL ALGORITHM FOR  
SEA SURFACE HEIGHT ESTIMATION  
USING COMPLEX SAR DATA

FINAL REPORT

Period: July 1, 1982 to December 31, 1983

NASA GRANT NAGW-387

Dr. Robert O. Harger  
Electrical Engineering Department  
University of Maryland  
College Park, Maryland 20742

1. The area of research of this grant was the study of a novel method of extracting sea height information - the sample functions, generally - from SAR complex data, a method that was suggested by a fundamental SAR ocean imaging model for gravity waves[1], that showed that information about the long wave is present in the SAR complex data, especially its phase. The initial study [2],[3], mainly supported by earlier NASA and ONR grants and partially supported at the publication stage by the present grant, employed an ad hoc, albeit quite reasonable, phase demodulation algorithm followed by linear regression and filtering: only the latter two steps incorporated a priori information that might be available. A relatively simplified simulation indicated that, among other possible limitations, the finite bandwidth of the SAR system imposed the apparently most serious limitation. A preliminary application to SEASAT-SAR complex imagery was encouraging. This work has been reported to the community, formally and informally [2],[3],[4],[6]. It was evident that a priori information about the long wave, at a minimum, if incorporated into a "more sophisticated" phase demodulation structure - i.e., at an earlier point in the algorithm, could conceivably mitigate this bandwidth limitation.

2. The work on this grant began by directly addressing the following central problem: given the SAR complex data of the sea, modeled as described above, and received along with thermal noise, what is the optimal (minimum mean-square error) estimator (a conditional expectation, then) of the long wave structure and what is its performance? While such an estimator is generally very difficult to find and, when found, implement, nevertheless we have done so for this problem! The significance of

such an answer is simply that it gives the best possible performance whatever deleterious effects may be modelled - finite bandwidth, thermal noise, random phase, etc.

(a) In particular, it has been found that this optimal estimator is able to overcome, to a considerable degree, the bandwidth limitation encountered by the earlier-posed, ad hoc, sub-optimal estimator. The optimal estimator is able to do this because it incorporates in its structure the a priori knowledge available). This estimation structure can be quite flexibly adaptive (at the cost of increased computation), is realized as an efficient, recursive calculation - e.g., as inferred from the SAR image, and, generally speaking, seems practical.

While we will defer detailed discussion to a forthcoming article [8], we call attention to the simulation shown in Fig. 1. The complex image was (randomly) generated using our model of the SAR complex image of the sea and was processed by the optimal estimation structure to produce an estimate of the height of a sinusoidal long wave - of known phase and wavenumber, as could be separately estimated from the SAR image, e.g. the long wave shape is shown in Figure 1 and the resulting mean-square error, and its sample average, for 50 simulation runs is shown in Figure 2. The wavenumber spectrum generated by the SAR ocean-sensing mechanism is several times greater than the SAR bandwidth but the performance is very good!!

(Also shown for reference is the Cramer-Rao lower bound when the height is an unknown parameter: in the simulation it was assumed to be a Rayleigh random variable with an a priori known variance.)

(b) The above-discussed optimal model has, in the main, been elaborated so far assuming a stationary scene. Actually, it may well turn

ORIGINAL PAGE IS  
OF POOR QUALITY

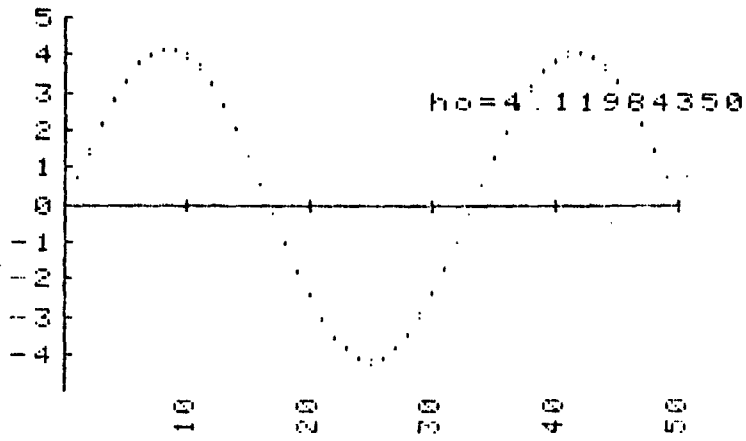


Fig. 1

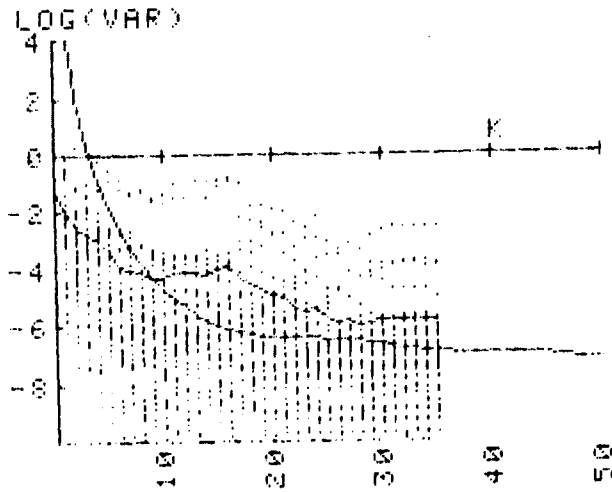


Fig. 2

out that the assumption was not especially limiting in view of analysis concerning the image model nature. Under reasonable conditions (e.g., an L-band SAR with not too fine a resolution and typical sea parameters) (i) the small wave structure part that can influence the SAR image is more concerted than dispersive in its action, and (ii) an appropriate focus adjustment can "render the long wave stationary". Then, with some details, the SAR imaging model reduces to that used in the above-discussed height estimation study.

(The observation (ii) is a well-known controversy in this community and we have had a fairly general proof that the focus adjustment is determined by the long wave's phase velocity for some time. The experimental "test" of this focus parameter dependence, proposed at an APL workshop last October was, as reported at a MARSEN workshop at JPL in January, in each instance supportive of our SAR model: that is, that the dependence is on the long wave's phase velocity.)

(c) In considering the practical implementation of this optimal estimator, it was noted that a significant saving in computation can be achieved by generating the short wave ensemble by a so-called "chaotic dynamical" process - rather than the "conventional" (e.g., Markov) random process models. Such an observation is of much wider consequence and an initial publication has been prepared [7]. Besides its potential computational advantage [8], such "chaotic" models of the sea surface are known to arise naturally as solutions to the nonlinear hydrodynamical equations and, hence, may be precisely the kind of models needed.

(d) The nature of the short wave ensemble plays a critical role: its presence is necessary for receipt of backscattered energy at typical intermediate incidence angles; at small incidence angles a quasi-specular

backscatter from the long wave can be more significant. The structure of an optimal height estimator, and its performance depends upon the statistical nature - e.g., "coherence length" - of the short wave ensemble and on the backscatter mode as determined by the incidence angle. A simulation of the estimation algorithm - and the SAR image - in a study would be very informative, as would be eventual comparison with the data forthcoming from the SIR-B experiment, offering data at various incidence angles.

(e) The algorithm was simulated through numerical simulation of the optimal estimation algorithm to establish, as completely as possible, its accuracy, flexibility, and practicality; The attempt to apply the algorithm to SEASAT-SAR data, as supplied by NASA JPL and/or ERIM, was only partially accomplished: despite repeated requests to both, only a limited amount of data was obtained from ERIM: see [8], included in this report.

3. The following publications, presentations, and discussions - accomplished and prospective - have been done during the Grant period. (It is likely that the topic of [8] will produce several publications - as, e.g., [7].)

I. Journal, book, and proceedings publications supported by the Grant:

- (1) "The SAR image of short gravity waves on a long gravity wave", in Proceedings of a Symposium on Wave Dynamics and Radio Probing of the Ocean Surface, O. M. Phillips and K. Hasselman, Eds., Plenum Press (in press). (Partial support of revision and manuscript preparation; also supported by earlier NASA grant.)



- (2) "A sea surface height estimator using synthetic aperture radar complex imagery", IEEE Trans. Ocean Engineering, April 1983.  
(Partial support for revision and manuscript preparation; also supported by earlier NASA grant.)
- (3) "A sea surface height estimator using SAR complex imagery", Proceedings of Oceans '82 Conference, Washington, DC September 1982. (Partial support for travel and manuscript preparation; also supported by earlier NASA grant.)

## II. Workshop participation related to grant:

- (4) "A novel SAR spectral estimation algorithm", presented at SEASAT-SAR Workshop on Ocean Wave Spectra, Johns Hopkins Applied Physics Laboratory, October, 1982.
- (5) ONR Workshop on SAR Ocean Imaging Applications, Johns Hopkins Applied Physics Laboratory, December, 1982.
- (6) NASA MARSEN Workshop on SAR Ocean Imaging Theory and Experiment, Cal. Tech. JPL, Jan., 1983.
- (7) "Optimal estimation with chaotic dynamics", Proceedings of the 1983 Conference on Information Sciences and Systems, Johns Hopkins University, March, 1983.

## III. Publications in process:

- (8) "A Fundamental Model and Efficient Inference for SAR Ocean Imagery", being revised for publication in IEEE Jo. Oceanic Engrg.

Enclosed are a reprint of [7] and a preprint of [8].

Professor Robert O. Harger  
Electrical Engineering Department  
University of Maryland  
College Park, MD 20742

## SUMMARY

Recently deepening understanding of nonlinear dynamical systems has revealed an interesting aspect of their possibly complicated behavior - their so-called 'chaotic', seemingly random, evolution. The observation of such an evolution leads naturally to the problem of estimating aspects of such systems, a problem area of increasing importance as the use of such models spreads into many sciences.

While the evolution of chaotic systems can be very complex, it is the result of iterating a nonrandom mapping of a (possibly random) initial state: optimal estimation structures can thereby simplify, relative to conventional random evolutions, possibly to practicality in specific instances.

This last remark is of additional significance since, in practice, it is often true that only quite limited knowledge is available for model construction - e.g., a correlation function: the 'orbits' of a chaotic dynamical model may well have a suitable sample-path correlation.

Typically, the evolution of such chaotic dynamical systems is indexed by a 'chaos parameter': both the gross and detailed nature of the evolution can depend upon its precise value. Thus a computationally simple dynamical model is capable, under parametric control, of generating a diversity of 'sample functions'. Of course, the obverse is that, first,

care must be taken in applying such models and, second, the performance of estimation schemes may also sensitively depend upon the value of the chaos parameter.

The formulation of a recursive estimation problem, in discrete time, using Markov and chaotic descriptions is contrasted. Then a simple parameter estimation problem is noted in which the more general role of certain orbit functionals appears. Next a more complicated nonlinear filtering problem - arising, e.g., in an ocean remote sensing system - is discussed. Finally, the 'identification' of the chaos parameter itself is studied, assuming an a priori distribution. Generally conditional expectation estimators are considered with the assistance of numerical computation.

Abstract

Nonlinear mappings that can exhibit "chaotic," seemingly random, evolution have appeal as models of dynamical systems. Their deterministic evolution, vis-a-vis Markov evolutions, can result in much simpler optimal detection and estimation algorithms. The variation of a "chaos" parameter ( $\mu$ ) can result in diverse evolutions, suggesting a simple but rich source of model variations. For the specific mapping examined here, this latter possibility is problematic due to the extreme sensitivity on  $\mu$  of the evolution in the "chaotic regime."

1. Introduction

Recent deepening understanding of nonlinear systems has revealed an interesting aspect of their possibly complicated behavior - their so-called "chaotic," seemingly random, evolution. The observation of such an evolution leads naturally to the problem of making inferences regarding aspects of such evolutions, a problem increasing in importance with the spreading study of such models in many scientific areas.

While the evolution of such a system can be very complicated indeed in detail, in one respect it is simple, evolving as an iterated, nonrandom mapping on a given initial state. Optimal algorithms for inference - detection and estimation - can be computationally quite feasible.

This observation and the remark that, in practice it is often true that only quite limited knowledge - e.g., a covariance function - is available for model construction, leads to the idea that a nonlinear, "chaotic" model might provide evolutions with suitable properties.

Such chaotic dynamical models may be indexed by a "chaos" parameter: both the gross and detailed nature of the evolution may depend dramatically upon its precise numerical value. Thus a relatively simple dynamical model can be capable of generating a diversity of evolutions, under a simple parametric control. Paradoxically, careful consideration would be required in a practical application. Also, the performance of optimal inference algorithms may depend sensitively on this parameter. Both matters will be addressed here.

2. Markov and Chaotic Inference Models

(a) Consider a discrete time, nonlinear system evolving in accordance with the dynamical model

$$x(k+1) = f[x(k), \omega(k)], \quad k=0, 1, \dots, \quad (1)$$

where  $\{\omega(k)\}$  is a sequence of mutually independent random variables ("r.v.s"). The evolution (1) is observed as

$$y(k) = g[x(k), v(k)], \quad k=0, 1, \dots, \quad (2)$$

where  $\{v(k)\}$  is a sequence of mutually independent r.v.s, the random processes  $\{\omega(k)\}$  and  $\{v(k)\}$  being independent. ( $f$  and  $g$  are real functions of two real arguments.)

Taking up, e.g., the filtering problem - an optimal estimation of  $x(k)$  given the observation  $y(k) \equiv (y(0), \dots, y(k))$ , the knowledge sufficient for estimating  $x(k)$  in accordance with common optimality criteria - e.g., minimizing the estimate's mean-square error ("MSE") - is given by the a posteriori distribution of  $x(k)$  given  $y(k)$ , denoted  $\rho(x(k) | y(k))$ . (We assume density functions ("d.f.s") exist in every case.) It is well-known that the evolution of this a posteriori d.f. is governed by the recursion

$$\rho[x(k+1) | y(k+1)] = \frac{\int F(k+1, k) dx(k)}{\int F(k+1, k) dx(k) dx(k+1)}, \quad (3a)$$

where

$$F(k+1, k) \equiv \rho[y(k+1) | x(k+1)] \rho[x(k+1) | x(k)] \rho[x(k) | \vec{y}(k)]. \quad (3b)$$

It is also well-known that this recursion is, generally, very difficult to specify in detail and implement as a feasible computation. The minimum MSE estimator ("M-MSE-E") of  $x(k)$ , given  $y(k)$ , is then

$$\hat{x}(k | k) = \int x(k) \rho[x(k) | \vec{y}(k)] dx(k) \quad (3c)$$

where  $\rho[x(k) | \vec{y}(k)]$  is computed recursively by (3a).

(b) Alternatively, consider the evolution of a possibly "chaotic" nonlinear system defined by

$$x(k+1) = f_{\mu}[x(k)], \quad k=0, 1, \dots, x(0) = x_0, \quad (4)$$

where  $x_0$  is an initial state and  $\mu$  is a ("chaos") parameter;  $x_0$  and/or  $\mu$  may be random variables ("r.v.s"). Conditioned upon any such randomness, if present, (4) describes a nonrandom evolution that, when replacing (1) as a dynamical model, results in a great simplification of (3), namely

$$\rho[x(k+1) | \vec{y}(k+1)] = \quad (5a)$$

$$\frac{\int \int \rho[y(k+1) | x(k+1)] \delta[x(k+1) - f_{\mu}^{k+1}(x_0)] G(k) dx_0 d\mu}{\int \int G(k+1) dx_0 d\mu}$$

\*Research supported by NASA Grant NAGW-387.

where (5b)

$$G(k) = \rho \{ y(k) | x(k) = f_{\mu}^k(x_0) \} G(k-1), G(0) = \rho(x_0) \rho(\mu).$$

Here  $x(k) = f_{\mu}^k(x_0)$  is the  $k$ -th iterate of  $f_{\mu}$ ,  $f_{\mu}^0(x_0) = x_0$ .

Thus, e.g., the M-MSE-E of  $x(k)$ , given  $\vec{y}(k)$ , is

$$\hat{x}(k|k) = \int \int f_{\mu}^k(x_0) G(k) dx_0 d\mu / \int G(k) dx_0 d\mu. \quad (5c)$$

A variety of related inference problems can be posed, all simplifying greatly as a consequence of the simplification of the joint d.f.:

$$\rho(\vec{y}(k), \vec{x}(k|\mu)) = \prod_{i=0}^k \rho(y(i) | x(i)). \quad (5d)$$

$$\prod_{j=1}^k \delta(x(j) - f_{\mu}^j(x_0)) \cdot \rho(x_0) \rho(\mu).$$

(c) The model (4) can result in far less calculation than the model (1). Suppose  $x(k|k)$  at  $k=k_*$  is required: (3c) requires  $4k_*$  integrations; in contrast, (5c) requires only 4. If  $x(k)$  in model (1) is a vector of dimension  $N$ , the integrations required are, resp.,  $4k_*N$  and 4. This latter comparison is of interest if, in such a case, (4) can, in some sense, adequately replace (1) as a model.

(d) For the specific numerical calculations here we choose the mapping

$$f_{\mu}(x) = 1 - \mu x^2, \quad x \in [-1, 1], \mu \in [0, 2]; \quad (6)$$

it is representative of a well-studied class of mappings that are (i) continuous, (ii) of one maximum (at  $x=0$ ), (iii) monotone decreasing with increasing  $|x|$ , and (iv) of a certain convexity in the derivative  $\partial f / \partial x$  [1]. The general nature of the "orbits"  $\{x(k) = f_{\mu}^k(x_0), k > 0\}$  is suggested by Fig. 1 where  $\{x(k), k=500 \text{ to } 600\}$  is plotted versus  $\mu$ . Viewing it, some of the following facts are agreeable.

Fig. 1-The iterates (500 to 600) of (6).

For sufficiently small values of  $\mu$ , the

orbits, for almost all  $x_0$ , approach a "final" value  $x(\infty)$ , a fixed point of the mapping  $f_{\mu}$ . As  $\mu$  is increased sufficiently, a "bifurcation" occurs, the orbit then, for almost all  $x_0$ , approaching a stable, periodic visit to two values, fixed points of the mapping  $f_{\mu}^2$ . As  $\mu$  increases, further bifurcations occur on an increasingly finer scale, until  $\mu = 1.40155\dots$  is reached, where a quite different behavior is encountered.

There an aperiodic motion on a set of (Lebesgue) measure 0 occurs; the orbits of almost all  $x_0$  are attracted to this set, and the orbits initially "close" remain close (for almost all  $x_0$ ) - an ergodic, but not mixing, evolution.

When  $\mu=2$ , the orbits are also almost all aperiodic, but range over the entire interval  $[-1, 1]$ : an invariant measure, absolutely continuous with respect to Lebesgue measure, exists and its form is known [2]. Orbits initially close almost surely do not remain close - an ergodic and mixing evolution. (Incidentally, the points  $x_0=0, \pm 1/2, \pm 1$  are easily directly seen to be exceptional points - as a numerical analysis may well inadvertently discover!)

It is not known if other types of evolution occur: in fact, the dynamics of this model are not fully understood, though a great deal is known [1]. The following facts are helpful in orienting and evaluating numerical analysis. (i)  $f_{\mu}$  has either one or no stable, periodic orbit. (ii) If  $f_{\mu}$  has a stable, periodic orbit, then the orbits of almost all  $x_0$  are attracted to it and, specifically,  $x_0=0$  is so attracted.

### 3. A simple estimation problem

A typical question that arises concerning the nonlinear model (4) occurs in the following simple estimation problem. Suppose that  $x_0$  and  $\mu$  are known a priori and that (2) is specialized to

$$y(k) = a x(k) + v(k), \quad k=0, 1, \dots, \quad (7)$$

where  $a$  is an unknown parameter to be estimated, having data  $v(k)$ . Suppose further that the  $\{v(k)\}$  are identically distributed normal r.v.s. with mean 0 and variance  $\sigma^2$ .

Then it is easy to show that the maximum likelihood estimator,

$$\hat{a}(k) = \left[ \sum_{i=0}^k y(i) f_{\mu}^i(x_0) \right] / \left( \sum_{i=0}^k [f_{\mu}^i(x_0)]^2 \right), \quad (8a)$$

is efficient - that is, it is unbiased and of error variance equal to the Cramer-Rao lower bound, namely

$$E\{[\hat{a}(k) - a]^2\} = \sigma^2 \left\{ \sum_{i=0}^k [f_{\mu}^i(x_0)]^2 \right\}^{-1}. \quad (8b)$$

Therefore, of special interest is the average along the orbit,

$$V(k; x_0, \mu) = \frac{1}{k} \sum_{i=0}^k [f_{\mu}^i(x_0)]^2. \quad (8c)$$

Certain "standard" questions arise: e.g., for large  $k$ , does  $V(k; x_0, \mu)$  depend upon  $x_0$  and/or  $\mu$ ?

For the model (6),  $V(k; x_0, \mu)$  is easily numerically calculated. The result can be expected to be influenced by two phenomena: first, a number of iterations may be required before the orbit arrives on the "attractor" (assuming it exists) and, second, a very large number of iterations may be required to achieve "stable" average value over the attractor. The first effect is noticeable but here minimized by summing from the 100th iteration on. A sum over the subsequent 100 iterations resulted in an orbit average  $V$  apparently independent of  $x_0$  for trial values of  $\mu = .4, .8$ , and  $1.2$ : see Fig. 2 where  $x_0 = (0, 0.05, \dots, 1)$ . Further calculation over 1,000 (vice 100) iterations resulted in independence of  $x_0$  of  $V$  when  $\mu = 1.6$  and, when  $\mu = 2$ , further calculation over 5,000 iterations resulted in a stable value of  $V$ , independent of  $x_0$ .

Fig. 2-The orbit average  $V$  of (8c) versus  $x_0$ , with  $\mu$  as parameter

#### 4. Chaos Parameter Estimation

Taking up the "chaotic" dynamical model (4) and the observation model (6), (7) - with  $a=1$ , the M-MSE-E  $\hat{\mu}(k)$  of  $\mu$ , given data  $\vec{y}(k)$ , is, by (5),

$$\hat{\mu}(k) = \int \mu \rho(\vec{y}(k) | \mu) \rho(\mu) d\mu / \int \rho(\vec{y}(k) | \mu) \rho(\mu) d\mu \quad (9a)$$

where

$$\rho(\vec{y}(k) | \mu) = \frac{1}{\sqrt{2\pi} \mu} \exp\left\{-\frac{1}{2\mu^2} \sum_{i=0}^k [y(i) - f_{\mu}^i(x_0)]^2\right\}. \quad (9b)$$

The sums are efficiently, recursively calculated.

The dynamical, observation, and optimal estimator equations were numerically simulated and some results are shown in Fig. 3, for  $\mu \in (0.33, 1, 1.46, 1.76)$ , all with  $x_0 = 0$ . Referring to Fig. 1, the rate of convergence for  $\mu \in (0.33, 1, 1.76)$  intuitively corresponds to the "distinctiveness" of these  $\mu$  values; the quite rapid convergence for  $\mu = 1.46$  in the chaotic region is informative. The (true value, estimate)-pairs

were  $(0.33, 0.332, \dots), (1, 1.01, \dots), (1.46, 1.45, \dots), (1.76, 1.763, \dots)$ , all for  $\nu = 0.1$ . These simulations employed a net of 100 points in  $\mu$ : as  $k$  increased, the support of the posteriori d.f.  $\rho(\mu | \vec{y}(k))$  became, within the numerical range of the computer ( $10^{-435}$ ), confined to a small portion of these points;  $\therefore$ , a more refined, or adaptively refined,  $\mu$ -net would be of interest.

Fig. 3- The M-MSE-E  $\hat{\mu}$  of (9) for several  $\mu$ .

The general conclusion at this point is that the parameter  $\mu$  is efficiently and accurately estimated by the M-MSE-E. At issue, however, is a somewhat more subtle matter, as will be seen.

Cramer-Rao bound. - The Cramer-Rao lower bound on the mean-square error that any estimator may have, is of interest though it is not necessarily attainable by any estimator. This lower bound involves the generally well-known form-take  $x_0$  and  $\mu$  to be unknown parameters -

$$-E\left\{\frac{\partial^2}{\partial \mu^2} \ln \rho(\vec{y}(k) | \mu)\right\} = \frac{1}{\mu^2} \sum_{i=0}^k \left[\frac{\partial}{\partial \mu} f_{\mu}^i(x_0)\right]^2 \quad (10a)$$

Here, given (6), the derivative with respect to  $\mu$  can be defined recursively as

$$\frac{\partial}{\partial \mu} f_{\mu}^n = -(f_{\mu}^{n-1})^2 - 2\mu f_{\mu}^{n-1} \cdot \frac{\partial}{\partial \mu} f_{\mu}^{n-1}, \quad n \geq 1, \quad \frac{\partial}{\partial \mu} f_{\mu}^0 = 0. \quad (10b)$$

The behavior of  $\partial f^n / \partial \mu$  itself is of some interest: like  $f^n$ , it displays a rich behavior. While bounded-it is a polynomial in  $\mu$  of degree less than  $n$ , it can be relatively large at points (in  $\mu$ ) of bifurcation of  $f^n$ , and it is very large in the "chaotic region." In Fig. 4, the 90th through 100th iterates of this derivative are plotted over a restricted  $\mu$ -set in the "chaotic" regime so that detail may be seen. It can be many orders of magnitude greater still at larger  $\mu$ . At least some of the nature of  $\partial f^n / \partial \mu$  is inferable from the nature of  $f^n$  as evidenced in Fig. 1.

ORIGINAL PAGE IS  
OF POOR QUALITY

ORIGINAL PAGE IS  
OF POOR QUALITY

Fig.4 - The derivative  $\partial f^n / \partial \mu$  of (10b), for  $n = 90$  to  $100$ , versus  $\mu$ .

The orbit average appearing in (10a),

$$\langle k \rangle \equiv \frac{1}{k} \sum_{i=0}^k \left[ \frac{\partial}{\partial \mu} f_{\mu}^i(x_0) \right]^2 \quad (10c)$$

is shown in Fig. 5 for  $k=20$ ,  $x_0=0.05$ , and 40 points in  $\mu$ . As the number of  $\mu$  points are increased, greater detail in  $\langle k \rangle$ 's dependence on  $\mu$  is seen in the chaotic region, generally to the limit of the computer graphics and beyond. The nature of the  $\mu$ -dependence otherwise is intuitively agreeable with the dependence exhibited in Figs. 1 and 4.

Fig.5-The orbit average (10c) appearing in the Creamer-Rao bound.

The very large values of  $\langle k \rangle$ , for this relatively small  $k$ , for most of the  $\mu$  in the chaotic region, seem to there allow extremely accurate estimation of  $\mu$ . (A Monte Carlo simulation of the M-MSE-E (9) could establish, numerically, whether or not such estimators exist.) But such a conclusion would depend upon the utilization of the estimate: if it is to be able to "identify", or fix, the chaotic dynamical system so that the orbit, and its attendant properties - e.g., orbit

correlation function - would then be known, the conclusion appears to be unjustified! To clarify this, sharper measures of "orbit distinguishability" are now considered.

### 5. Orbit distinguishability

(a) The results of the chaos parameter estimation problem just discussed allowed the possibility that the orbits of (6), as observed via (7) (with  $a=1$ ), are extremely distinguishable. To sharpen this question, suppose one of two orbits, corresponding to  $\mu_1$  and  $\mu_2$ , are accordingly observed: then, by any of the usual decision criteria, the decision performance is determined by the "distance"

$$\|f_{\mu_1}^k(x_0) - f_{\mu_2}^k(x_0)\|^2 = \sum_{k=0}^k |f_{\mu_1}^k(x_0) - f_{\mu_2}^k(x_0)|^2, \quad (11)$$

normalized by  $\nu^2$ .

In Fig. 6 is shown this distance, depending on a sequence  $\mu_2 \equiv \mu_1 - (0.1)^i$  with  $\mu=1.6$  and for an orbit segment from  $k=100$  to  $1,100$ . The remarkable result is that, to the accuracy of the computer's representation of numbers (12 significant digits), the orbits remain distinguishable!

Fig.6- The distance (11) between orbits of  $f_{\mu_1}$  and  $f_{\mu_2}$ ,  $\mu_2 = \mu - (0.1)^i$ .

(b) Another measure of distinguishability of the orbits is the "orbit correlation coefficient"

$$\rho_{1,2} \equiv \frac{\sum_{k=K_{\min}}^{K_{\max}} f_{\mu_1}^k(x_0) f_{\mu_2}^k(x_0)}{\|f_{\mu_1}^k(x_0)\| \cdot \|f_{\mu_2}^k(x_0)\|} \quad (12)$$

Referring to Fig. 7, it is seen that this same extreme distinguishability persists to the limit of machine accuracy. (The values of unity for  $\rho$  near 12 occur when the machine can no longer distinguish  $\mu_1$  and  $\mu_2$ .) At the same time the correlation with orbits considerably removed in  $\mu$  persists. (As a check on the hoped-for independence of the calculation on  $x_0$ , the curve

of Fig. 7 is actually the overlay of the curves for  $x_0=0.1$  and  $x_0=0.5$ : they are indistinguishable on the graphics display.)

## ORIGINALITY OF OF FOUR QUALITY

Fig. 7- The correlation coefficient  $\rho$  of (12) between orbits  $f_{\mu}$  and  $f_{\mu_2}$  for  $\mu_2 = \mu - (1/10)^L$ .

(c) Spectral density distinguishability.- It might be thought that, if a more gross property of the orbits were compared, their distinguishability might be smoother and decreasing with decreasing  $\mu$ -separation. Further, it is the orbit spectral density that is prospectively most useful for choice of a chaotic model in practice.

Given an appropriate segment of an orbit, we define the "orbit covariance function, o.c.f." as

$$R_{\mu}(t) \equiv \frac{1}{(K_{\max} - K_{\min})} \sum_{k=K_{\min}}^{K_{\max}} f_{\mu}^{k+t}(x_0) f_{\mu}^k(x_0),$$

$$t=0, \pm 1, \dots, L,$$

where  $K_{\min} - L > 0$ . (In order to allow the orbit to "stabilize", one prefers  $K_{\min} - L \gg 1$ , in fact: here,  $K_{\min} - L \approx 100$  would be satisfactory, generally.)

The "orbit spectral density, o.s.d." is defined as the discrete Fourier transform ("DFT") of the o.c.f.:

$$S_{\mu}(\omega) \equiv \sum_{t=L}^{+L} e^{-i\omega t} R_{\mu}(t), \quad \omega=0, \pm 1, \dots, \pm L, \omega \equiv 2\pi/(2L+1)$$

The "distinguishability" of  $S_{\mu_1}$  and  $S_{\mu_2}$  is defined as the distance

$$D_S(\mu_1, \mu_2) \equiv \frac{1}{2L+1} \sum_{\omega=-L}^{+L} |S_{\mu_1}(\omega) - S_{\mu_2}(\omega)|^2, \quad (13)$$

which is readily seen to be

$$D_R(\mu_1, \mu_2) \equiv \sum_{t=-L}^{+L} [R_{\mu_1}(t) - R_{\mu_2}(t)]^2,$$

a distance between o.c.f.'s, rather than, as earlier, a distance between orbits themselves. Writing this form out,

$$D_R(\mu_1, \mu_2) = \sum_{t=-L}^L \left\{ \frac{1}{\Delta K} \sum_{k=K_{\min}}^{K_{\max}} [f_{\mu_1}^{n+t}(x_0) f_{\mu_1}^k(x_0) - f_{\mu_2}^{k+t}(x_0) f_{\mu_2}^k(x_0)] \right\}^2, \quad \Delta K \equiv K_{\max} - K_{\min}.$$

In Fig. 8 this distance is shown for a sequence  $\mu_2 = \mu_1 - (1/10)^L$  approaching  $\mu_1 = 1.6$  in the "chaotic region," for  $K_{\max} = 200$ ,  $K_{\min} = 100$ ,  $L = 25$ ,  $x_0 = 0$ . Again, to the computer's limit of 12 significant digits, the orbit spectral densities are indistinguishable!

Fig. 8- The distance (13) between orbit spectral densities of  $f_{\mu}$  and  $f_{\mu_2}$  for  $\mu_2 = \mu - (1/10)^L$ .

(d) This extreme sensitivity of the orbit of (6), and its orbit correlation function, to the precise value of the parameter  $\mu$  in the chaotic region renders problematic the feasibility of using such a model in a practical case. Indeed, it raises a serious question whether the oft-cited and much-studied nonlinear mapping (6) is useful as a physical model at all.

### 6. References

1. P. Collet and J. P. Eckmann, Iterated Maps on the Interval as Dynamical Systems. Boston: Birkhauser, 1980.
2. S. M. Ulam and J. V. Neumann, "On combinations of stochastic and deterministic processes," Bull. Amer. Math. Soc. **53**, p. 1120 (1947).